Title: Acinar cell carcinoma of the pancreas with thyroid-like follicular features: first description of a new diagnostic challenging subtype.

Authors: Saglietti C, Schneider V, Bongiovanni M, Missiaglia E, Bisig B, Dorta G, Demartines N, Sempoux C, La Rosa S

Journal: Virchows Archiv : an international journal of pathology

Year: 2019 Jul 23

DOI: 10.1007/s00428-019-02628-3

Acinar cell carcinoma of the pancreas with thyroid-like follicular features. First description of a new diagnostic challenging subtype

[1]Chiara Saglietti, [1]Vanessa Schneider, [1]Massimo Bongiovanni, [1]Edoardo Missiaglia, [1]Bettina Bisig, [2]Gian Dorta, [3]Nicolas Demartines, [1]Christine Sempoux, [1]Stefano La Rosa (ORCID: 0000-0003-1941-2403)

[1]Institute of Pathology, Lausanne University Hospital and University of Lausanne, Lausanne, Switzerland
[2]Department of Gastroenterology, Lausanne University Hospital and University of Lausanne, Lausanne, Switzerland
[3]Department of Visceral Surgery, Lausanne University Hospital and University of Lausanne, Lausanne, Switzerland.

Word count: 1893

Author for correspondence:

Stefano La Rosa, MD
Institute of Pathology
University Hospital
25 Rue du Bugnon
1011 Lausanne
Switzerland
Tel: +41 (0)21 3147162
Fax: +41 (0)21 3147115
e-mail: stefano.larosa@chuv.ch

ABSTRACT

Acinar cell carcinomas (ACCs) of the pancreas are a heterogeneous group of neoplasms showing a wide spectrum of morphological features including acinar, solid, glandular, and trabecular architecture. In addition, uncommon cytological aspects have recently been described and include oncocytic, spindle, clear, and pleomorphic cell types. This wide histological spectrum represents a challenge in the diagnostic task for pathologists. Molecular mechanisms involved in the onset and progression of ACCs are not completely known, but, in general, they differ from those observed in ductal adenocarcinomas or neuroendocrine neoplasms of the pancreas and frequently include alterations in the APC/β-catenin pathway. In the present paper, we describe a new variant of ACC showing thyroid-like follicular features and *CTNNB1* mutation. This phenotype needs to be included in the spectrum of morphological presentation of ACC.

Keywords: acinar cell carcinoma; pancreas; thyroid-like; differential diagnosis; morphology

Introduction

Pancreatic acinar cell carcinomas (ACCs) may show different architectural patterns of growth including acinar, solid, glandular, and trabecular structures. In addition, other uncommon cytological features have recently been described and include oncocytic, spindle, clear, and pleomorphic cell types and this wide histological spectrum gives rise to difficulties in the differential diagnosis with other pancreatic neoplasms [1-4]. In such instances, immunohistochemistry is an essential tool to demonstrate acinar-specific products including trypsin, chymotrypsin, amylase, lipase, and carboxyl ester hydrolase [4], the last also detected with the anti-BCL10 monoclonal antibody [5]. It is worth noting that antibodies directed against these different markers differ in terms of sensitivity [2, 5, 6]. Anti-lipase and anti-amylase antibodies detect a low percentage of cases (<30% and <10%, respectively) [2], while anti-chymotrypsin antibody about 70% of ACCs [6]. Anti-trypsin and anti-BCL10 antibodies show the best sensitivity detecting 96% and 85% of cases, respectively [2], but their simultaneous use identifies about 100% of cases [2, 5].

In the present paper, we describe the clinico-pathologic and molecular features of an ACC showing a thyroid-like architectural pattern, which has never been previously described.

Case report

A previously healthy 51-year-old man presented with back pain and weight loss of 10 kg over the last year. Contrast enhanced abdominal CT scan and MRI showed a well-circumscribed mass, located in the uncinate process of the pancreas. Pancreatic endoscopic ultrasound fine needle aspiration was performed and a diagnosis of adenocarcinoma, not otherwise specified (NOS), was rendered. The patient underwent pancreaticoduodenectomy. Four

months later, chemotherapy with gemcitabine and capecitabine was started and 33 months after surgery, the patient was alive free of disease.

Materials and Methods

Immunohistochemistry was performed on a Ventana Benchmark XT autostainer (Ventana Medical System, Tucson, AZ, USA) using the antibodies listed in Table 1.

A representative FFPE tissue block was used for gene mutation, and rearrangement analysis. For mutation analysis by Next Generation Sequencing (NGS), an amplicon-based DNA library was prepared using a customized primer panel targeting 218 hotspot regions of 52 cancer genes (custom Ion AmpliSeq panel, Ion Torrent, Thermo Fisher Scientific, Waltham, MA, USA), and subsequently sequenced on an Ion Personal Genome Machine (PGM, Ion Torrent). For rearrangement analysis, the Archer FusionPlex Lung Kit (ArcherDX, Boulder, CO, USA) was applied to identify fusions involving 14 genes, including *BRAF.* This NGS technology allows the detection of chimeric transcripts even without prior knowledge of fusion partners or breakpoints. Starting from 200 ng RNA, the library was prepared according to manufacturer's instructions and sequenced on a MiSeq instrument (Illumina, San Diego, CA, USA). Furthermore, for *RET* and *PPAR*γ gene rearrangements, interphase fluorescence *in situ* hybridization (FISH) assays were performed on 4μm-thick sections using break-apart probes (Zyto*Light* SPEC RET Dual Color Break Apart Probe, ZytoVision, Bremerhaven, Germany; and Kreatech PPARG (3p25) Break FISH probe, Leica Biosystems, Nussloch, Germany), according to standard protocols.

Results

Fine needle aspiration of the mass yielded highly cellular smears comprising cohesive sheets and clusters of monomorphic cells, occasionally demonstrating glandular architecture. Amorphous eosinophilic colloid-like material was visible in the background or inside glandular lumens (Fig. 1A). Tumor cells were intermediate in size, polygonal, with finely granular cytoplasm. Nuclei were mostly round, regular, with smooth contour, prominent nucleolus and granular chromatin. On cell block, tumor cells were arranged in regular glandular structures, whose lumens contained a PAS-positive amorphous material (Fig. 1B). Neoplastic cells showed diffuse expression of CK7 and CK19. Chromogranin A (Fig. 1C) and synaptophysin were focally positive. BCL10 and trypsin were negative in tumor cells, although the former was positive in the amorphous material (Fig. 1D).

At gross examination, the tumor was well-circumscribed measuring 4.3 x 4.0 x 3.2cm and the cut surface was white-to-yellow and had a lobulated appearance.

Histologically, the tumor displayed follicular structures of varying sizes filled with amorphous, eosinophilic, PAS-positive colloid-like material, strongly resembling thyroid tissue (Fig. 2A). Intratumor fibrous stroma was scant and extensive necrosis was lacking. At higher magnification, follicles were lined by cuboidal to columnar cells containing a moderate amount of finely granular eosinophilic cytoplasm. The nuclei were round to oval, with a granular chromatin and a single nucleolus (Fig. 2B); they displayed focal chromatin clearing and nuclear grooving. Perineural and vascular invasion were observed. Two out 35 peripancreatic lymph nodes were metastatic. Tumor cells were immunoreactive for CKAE1/AE3, CK7, CK19, EMA, CD10, α-methylacyl CoA racemase, hMLH1, hMSH2, hMSH6, and hPMS2. The immunoreactivity for trypsin and BCL10 was heterogeneous in the tumor. Indeed, tumor cells showed a patchy but intense positivity for trypsin and BCL10: about 40% were positive for BCL10 and 60% for trypsin. Interestingly, in areas where neoplastic cells

were negative, trypsin and BCL10 stained the PAS-positive colloid-like material (Fig. 2C-F). Synaptophysin (Fig. 2G) and chromogranin A were expressed in scattered cells (<30% of tumor cells), which sometimes were also positive for trypsin. TTF1, thyroglobulin, PAX8, CDX2, lipase, amylase, PSA, CK20, insulin, glucagon, somatostatin, and α-inhibin were negative. β-catenin showed preserved membrane positivity, but an additional nuclear accumulation of the protein was observed in several tumor cells, with variable intensity (Fig. 2H). The Ki67 proliferative index was counted at 30%.

NGS mutation analysis yielded a mean coverage of 1504X and revealed two missense mutations: a c.95A>T (p.D32V) mutation in exon 3 of *CTNNB1* (allele frequency of 83%) and a c.740A>G (p.K247R) mutation in exon 4 of *ABL1* (allele frequency of 9%). The other genomic regions investigated, including the hotspot regions of *KRAS*, *NRAS*, *HRAS*, *BRAF* and *TP53* genes, did not show any detectable mutation. Copy number variation (CNV) analysis based on local reads coverage obtained from NGS data showed low level gains at chromosomal regions 1q, 3, 5q, 7p, 10, 13q, and of a more significant copy number gain of 20q (around 6 copies per cell).

No fusion transcript was detected involving any of the 14 genes screened by NGS, including the *BRAF* fusions previously described in pancreatic ACCs [7].

FISH assays demonstrated a copy number gain of *RET* (10q11; 3 to 6 copies per nucleus) and *PPAR*γ (3p25; 2 to 4 copies), but did not evidence any rearrangement of these genes.

Discussion

Pancreatic ACCs are a heterogeneous group of neoplasms showing a wide spectrum of morphological features including acinar, solid, glandular, and trabecular architectural

patterns. In addition, other uncommon variants have been described and include oncocytic, spindle, clear, and pleomorphic cell types [2, 4].

We describe for the first time an ACC with striking histological features resembling a well-differentiated follicular neoplasm of the thyroid. This new subtype represents a challenging entity due to the peculiar morphological features and to the patchy expression of acinar cell markers. The latter characteristic may represent a major diagnostic pitfall, especially on cytological examination. Indeed, in our cytology specimens both trypsin and BCL10 were positive in the colloid-like material, but negative in tumor cells, leading us to miss the preoperative diagnosis of ACC. The lack of cytoplasmic immunoreactivity for both acinar cell markers was also observed in several areas of the tumor at histological examination. Indeed, their cytoplasmic immunoreactivity was mainly absent in areas where the intraluminal colloid-like material was strongly positive for both BCL10 and trypsin. This suggests that the enzymes-containing colloid-like material is actively secreted by tumor cells, which discharge their enzymes content, resulting, in turn, in the lack of cytoplasmic immunoreactivity. The secreted material accumulated within the lumens determined their dilatation, conferring a “thyroid-like” appearance.

The peculiar morphological features of the present case raised the possibility of a metastasis from a thyroid carcinoma, which was excluded as the tumor was negative for thyroglobulin and TTF-1. In addition, the patient did not have a previous history of thyroid cancer and thyroid lesions were not detected at radiological investigation. Cases of primary renal and breast carcinomas, liver cholangiocarcinoma, and hepatic neuroendocrine neoplasm morphologically resembling thyroid follicular neoplasms have been reported in the literature and in all of them the neoplastic cells were negative for thyroid markers [8-11].

The prognostic meaning of “thyroid-like” features in these cancers is not clear, since follow-up data are limited.

Another diagnostic issue was represented by the focal expression of neuroendocrine markers that may suggest the diagnosis of neuroendocrine neoplasm, especially in the cytology specimen. Scattered neuroendocrine cells are frequently observed in ACCs [2] and only when they represent at least 30% of the tumor tissue, the neoplasm is defined as mixed acinar-neuroendocrine carcinoma, a tumor type that belongs to the large group of mixed neuroendocrine-non neuroendocrine neoplasms (MiNENs) [12, 13].

The molecular profile of the present case included a c.95A>T (p.D32V) mutation in exon 3 of *CTNNB1,* a c.740A>G (p.K247R) mutation in exon 4 of *ABL1,* and a copy number gain of 20q. The other genes investigated, including *KRAS*, *NRAS*, *HRAS*, *BRAF* and *TP53* did not show any mutation. The lack of *RAS* and *BRAF* mutations is in line with literature data, which indicate that *KRAS* mutations are practically absent in ACCs and that *BRAF* mutations are exceedingly rare [4]. Furthermore, the presence of recurrent *BRAF* fusions has recently been described in over 20% of pancreatic acinar-type neoplasms [7]. In our analysis did not found such *BRAF* alterations nor other fusion genes. Thanks to the peculiar NGS technology used to search for fusion transcripts (i.e., Anchored Multiplex PCR or AMP), rearrangements involving *BRAF* with any other partner gene would have been detected, even if not previously reported. Regarding *TP53*, mutations in this gene have been described in about 12% of ACCs [4] and, when associated with loss of the other allele, are associated with worse survival [14]. Although alterations in the APC/β-catenin pathway are relatively frequent in ACCs, mutations in the *CTNNB1* gene have been described in only 7% of cases [15]. In the present case we found an activating mutation in exon 3 of *CTNNB1*: similarly to other alterations affecting the N-terminal region of β-catenin, this D32V substitution appears to

prevent full phosphorylation of the protein, thereby leading to its abnormal stabilization and nuclear accumulation [16], as observed in this case with immunohistochemistry. Nuclear expression of β-catenin has been described in SPN, which, however, are negative for BCL10 and trypsin. The mutation detected in *ABL1* has been reported in approximately 0.5% of healthy European population (ExAC database) and is probably of little functional interest. Moreover, the copy number gain observed at 20q is consistent with what has been reported in ACC in previous studies [17, 18]. In line with the pancreatic origin of the cancer, FISH analysis did not show rearrangements of *RET* and *PPARγ* genes, which are genes involved in the pathogenesis of thyroid carcinomas.

In conclusion, a new variant of ACC showing thyroid-like follicular features is described and it should be added to spectrum of morphological variability of ACC.

Compliance with ethical standard: This was performed in accordance with research policies approved by Lausanne University Hospital Institutional Review Board.

Funding: none.

Conflict of Interest: The authors declare that they have no conflict of interest.

Contributions: CS analyzed data and participated in writing the manuscript; VS performed the histological diagnosis; MB performed the cytological diagnosis and participated in writing the paper; EM and BB performed molecular analyses, analyzed data and participated in writing the paper; GD performed clinical investigations and endoscopic ultrasound fine needle aspiration; ND performed pancreaticoduodenectomy; CS performed histological diagnosis, analyzed the data and participated in writing the manuscript. SLR conceived and designed the study, performed histological diagnosis, analyzed the data and wrote the manuscript. All authors critically reviewed the manuscript and gave final approval.

References

1. Klimstra DS, Hruban RH, Klöppel G, Morohoshi T, Ohike N (2010) Acinar cell neoplasms of the pancreas. In: Bosman FT, Carneiro F, Hruban RH, Theise ND (eds) WHO classification of tumours of the digestive system, 4th edn. IARC Press, Lyon, pp 314-318.
2. La Rosa S, Adsay V, Albarello L, et al (2012) Clinicopathologic study of 62 acinar cell carcinomas of the pancreas: insights into the morphology and immunophenotype and search for prognostic markers. Am J Surg Pathol 36:1782-1795.
3. Basturk O, Klimstra DS (2012) Acinar cell carcinoma of the pancreas and related neoplasms: a review. Diagn Histopathol 18:8-16.
4. La Rosa S, Sessa F, Capella C (2015) Acinar cell carcinoma of the pancreas: overview of clinicopathologic features and insights into the molecular pathology. Front Med 2:41.
5. La Rosa S, Franzi F, Marchet S, et al (2009) The monoclonal anti-BCL10 antibody (clone 331.1) is a sensitive and specific marker of pancreatic acinar cell carcinoma and pancreatic metaplasia. Virchows Arch 454:133-142.
6. Ordóñez NG (2001) Pancreatic acinar cell carcinoma. Adv Anat Pathol 8:144-159.
7. Chmielecki J, Hutchinson KE, Frampton GM, et al (2014) Comprehensive genomic profiling of pancreatic acinar cell carcinomas identifies recurrent RAF fusions and frequent inactivation of DNA repair genes. Cancer Discov 4:1398-1405.
8. Amin MB, Gupta R, Ondrej H, et al (2009) Primary thyroid-like follicular carcinoma of the kidney: report of 6 cases of a histologically distinctive adult renal epithelial neoplasm. Am J Surg Pathol 33:393-400.
9. Tosi AL, Ragazzi M, Asioli S, et al (2007) Breast tumor resembling the tall cell variant of papillary thyroid carcinoma: report of 4 cases with evidence of malignant potential. Int J Surg Pathol 15:14-19.

10. Chable-Montero F, Shah B S A, Montante-Montes de Oca D, et al (2012) Thyroid-like cholangiocarcinoma of the liver: an unusual morphologic variant with follicular, trabecular and insular patterns. Ann Hepatol 11:961-965.

11. Ibrahim ME, Abadeer K, Zhai QJ, et al (2017) Primary Hepatic Neuroendocrine Tumor with Unusual Thyroid Follicular-Like Morphologic Characteristics. Case Rep Pathol 2017:7931975.

12. La Rosa S, Sessa F, Uccella S (2016) Mixed neuroendocrine-nonneuroendocrine neoplasms (MINENs): unifying the concept of a heterogeneous group of neoplasms. Endocr Pathol 27:284-311.

13. Klöppel G, Couvelard A, Hruban RH, et al (2017) Neoplasms of the neuroendocrine pancreas: introduction. In: Lloyd Rv, Osamura RY, Klöppel G, Rosai J (eds) WHO classification of tumours of endocrine organs, 4th edn. IARC Press, Lyon, pp 211-214.

14. La Rosa S, Bernasconi B, Frattini M, et al (2016) TP53 alterations in pancreatic acinar cell carcinoma: new insights into the molecular pathology of this rare cancer. Virchows Arch 468:289-296.

15. Furlan D, Sahnane N, Bernasconi B, et al (2014) APC alterations are frequently involved in the pathogenesis of acinar cell carcinoma of the pancreas, mainly through gene loss and promoter hypermethylation. Virchows Arch 464:553-564.

16. Agaimy A, Haller F (2016) CTNNB1 (β-Catenin)-altered neoplasia: a review focusing on soft tissue neoplasms and parenchymal lesions of uncertain histogenesis. Adv Anat Pathol 23:1-12.

17. Bergmann F, Aulmann S, Sipos B, et al (2014) Acinar cell carcinomas of the pancreas: a molecular analysis in a series of 57 cases. Virchows Arch 465:661-672.

18. Jäkel C, Bergmann F, Toth R, et al (2017) Genome-wide genetic and epigenetic analyses of pancreatic acinar cell carcinomas reveal aberrations in genome stability. Nat Commun 8:1323.

Figure legends

Figure 1. Fine-needle aspiration cytology of the pancreatic tumor was hypercellular with abundant 3D clusters. Colloid-like material was visible in the background (arrow) (A). Sections obtained from the cell block showed well-formed micro and macrofollicular-like structures containing amorphous colloid-like material, which was also observed in the background. Tumor cells were of intermediate-size, polygonal, with finely granular cytoplasm. Nuclei were mostly round, regular, with smooth contour, prominent nucleolus and granular chromatin, with a mild degree of pleomorphism (B). Chromogranin A was focally intensely positive (C), and BCL10 was positive in colloid-like material, but not in tumor cells (D).

Figure 2. At low magnification, the tumor was characterized by follicular-like structures of varying sizes filled with amorphous, eosinophilic, colloid-like material strongly resembling thyroid tissue (A). At higher magnification follicle-like structures were lined by monotonous and regular cuboidal to columnar cells containing a moderate amount of finely granular eosinophilic cytoplasm. Their nuclei were round to oval, with a granular chromatin and a single nucleolus (B). In large areas of the tumor BCL10 was only positive in colloid-like material as observed in cytologic specimens (C). However, in other areas several cells showed cytoplasmic BCL10 immunoreactivity (D). Similar findings were observed for trypsin (E and F). Synaptophysin (G) was positive in less than 30% of cells and β-catenin showed

preserved membrane positivity, but an additional nuclear accumulation of the protein was observed in a significant number of tumor cells (H).

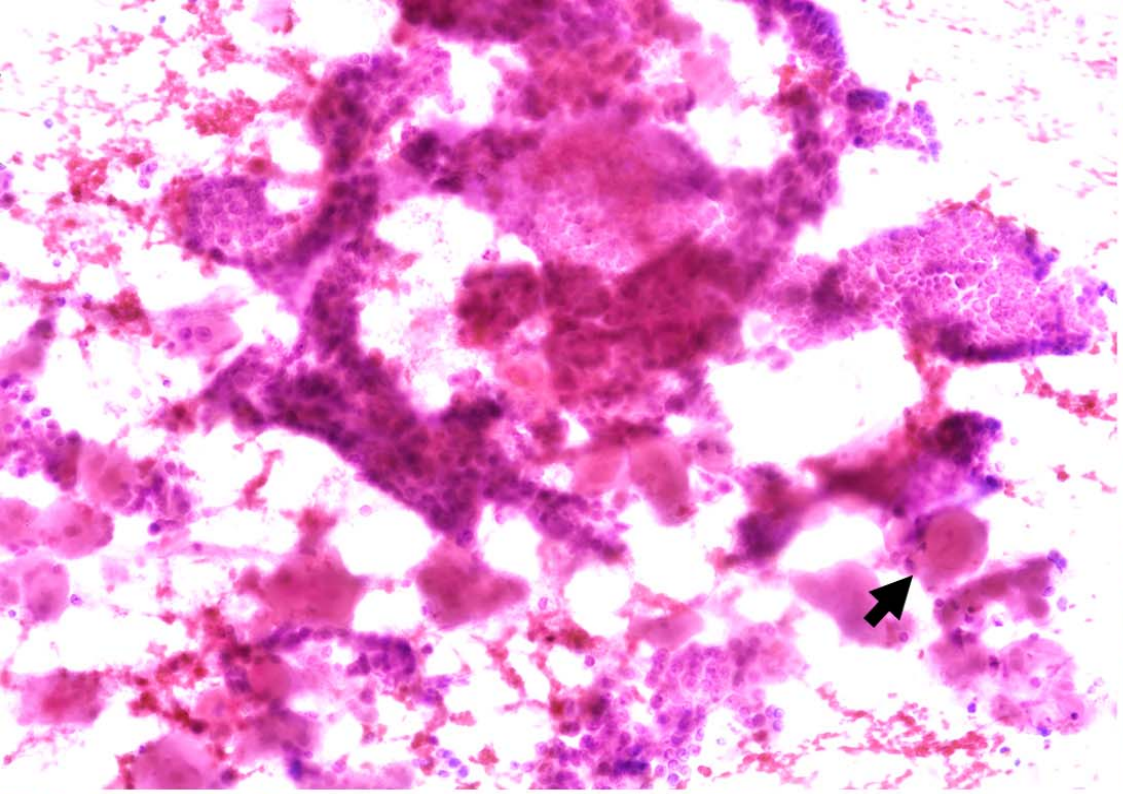

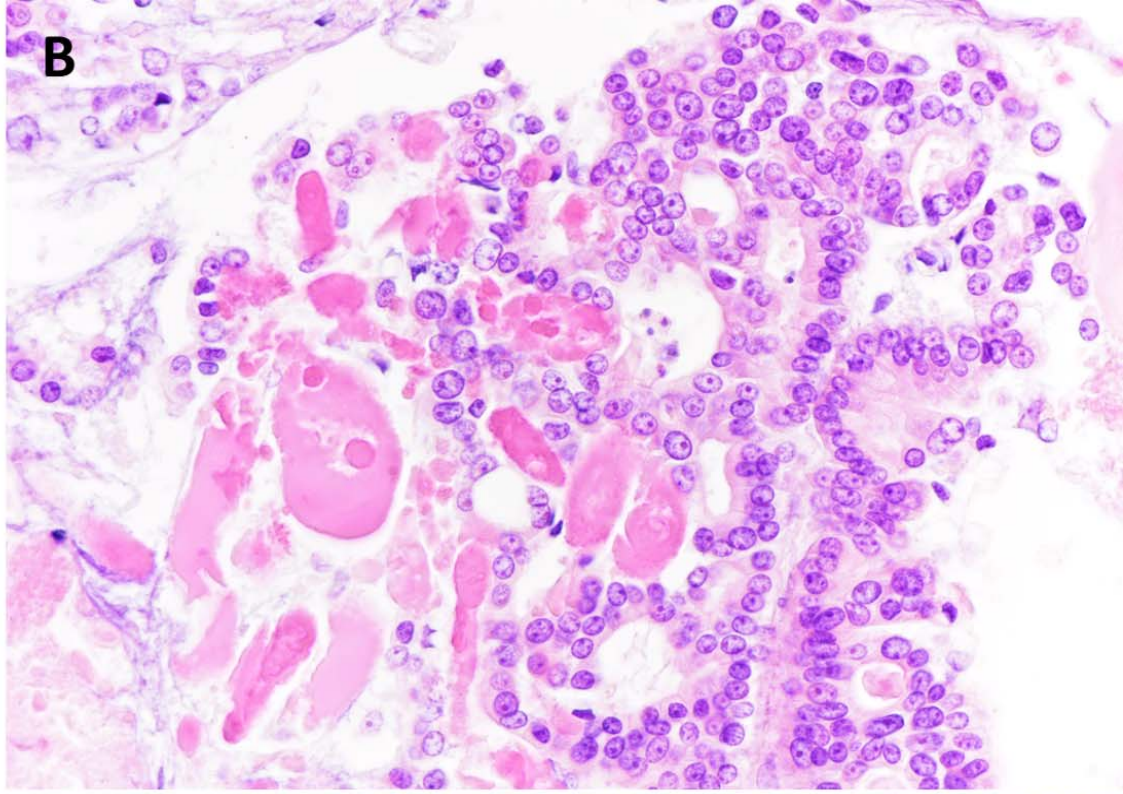
B

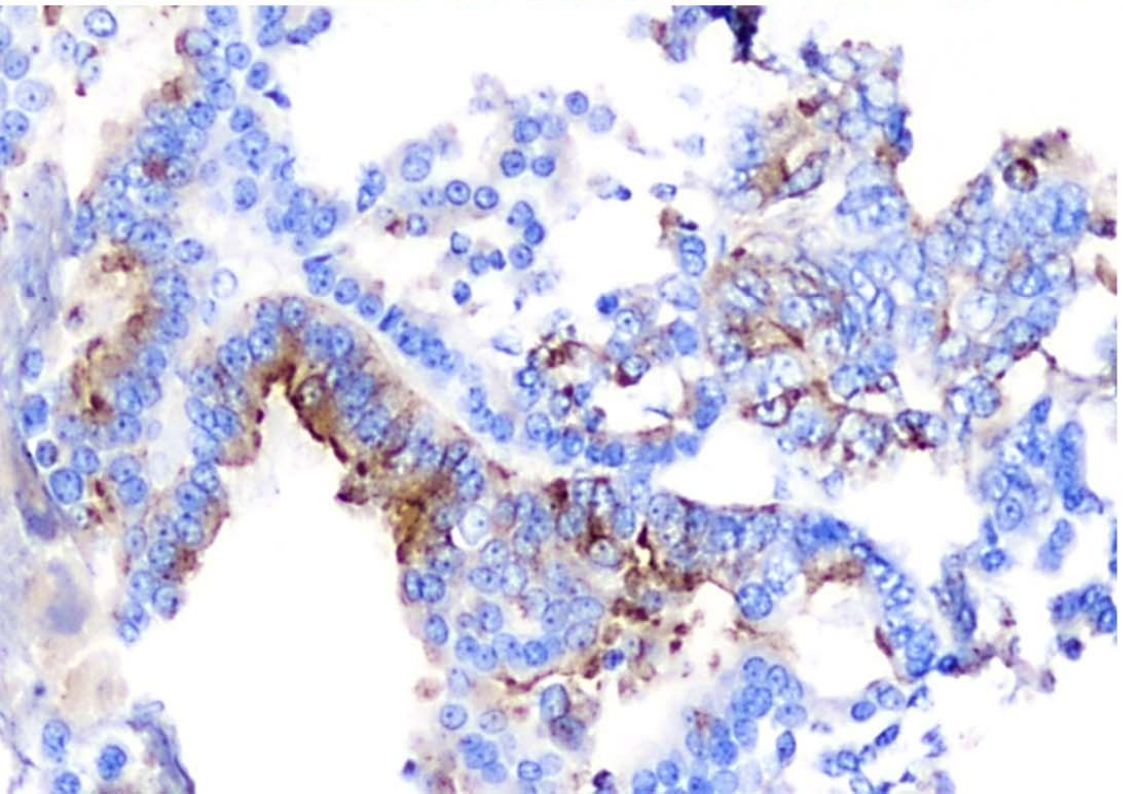

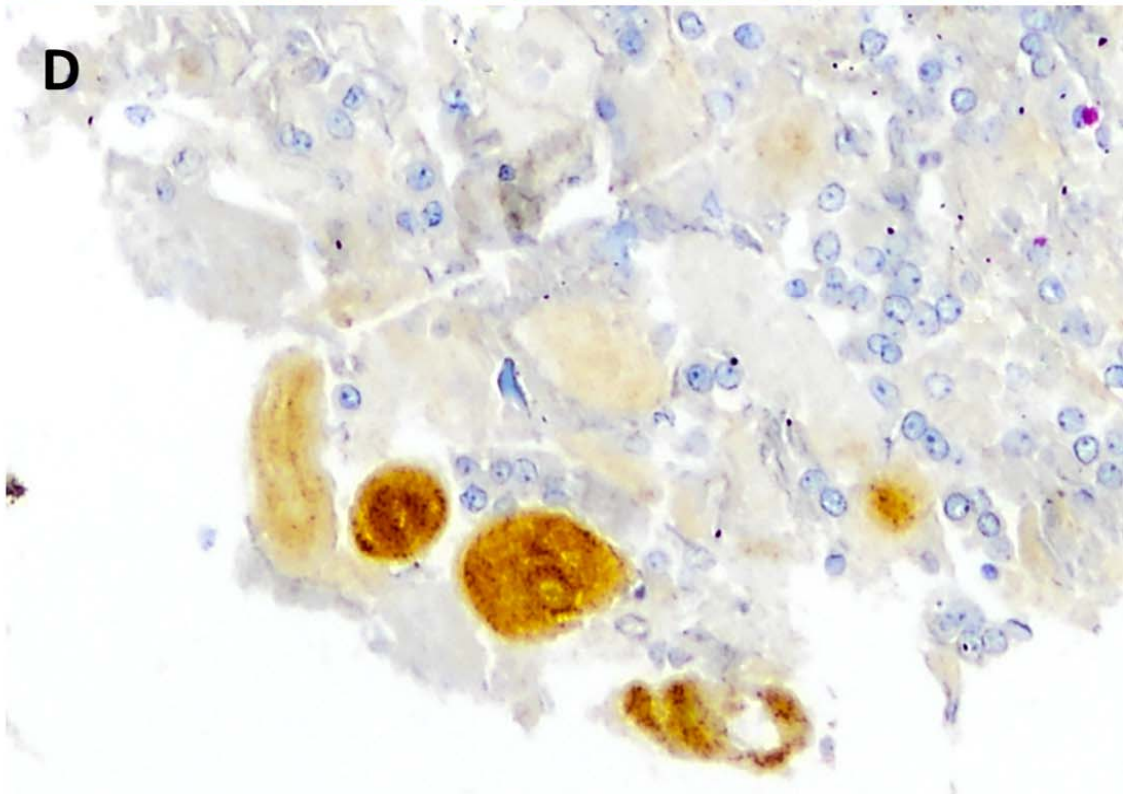
D

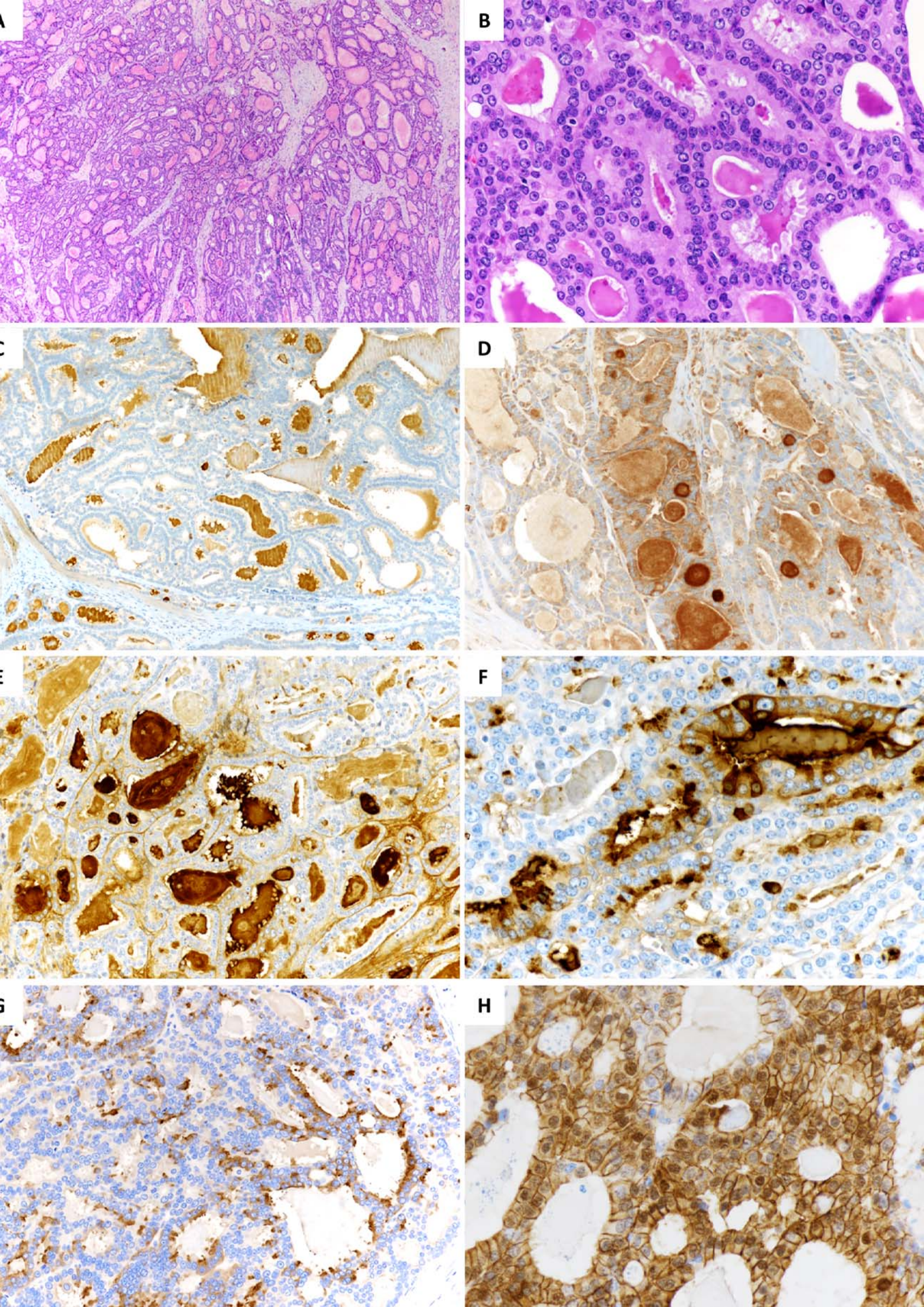
A
B
C
D
E
F
G
H

Table 1. Antibodies and antisera used.

Antibodies/antisera	P/M(Clone)	Dilution	Source
Trypsin	M(MAB1482)	1:100	Chemicon-Millipore International Inc., Temecula, CA, USA
BCL10	M(331.3)	1:300	Santa Cruz Biotechnology Inc., Santa Cruz, CA, USA
Amylase	M(6103)	1:2500	BioGenex Laboratories, San Ramon, CA, USA
Lipase	M(MAB1453)	1:1000	Chemicon-Millipore International Inc.
Cytokeratin	M(AE1/AE3)	1:5	Novocastra, Benton, UK
Cytokeratin 7	M(OV-TL 12/30)	1:200	Dako, Carpinteria, CA, USA
Cytokeratin 19	M(RCK108)	1:50	Dako
Cytokeratin 20	M(IT-Ks 20.8)	1:80	Progen Biotechnik, Heidelberg, Germany
EMA	M(E29)	1:100	Dako
Synaptophysin	M(27G12)	1:100	Novocastra
Chromogranin A	P	1:1000	Dako
Glucagon	P	1:500	Cell Marque, Rocklin, CA, USA
Insulin	P	1:200	Dako
Gastrin	P	1:1000	Dako
Somatostatin	P	1:3000	Dako
CD10	M(56C6)	1:50	Novocastra
PAX8	P	1:200	Proteintech, Rosemont, IL, USA
Thyroglobulin	M(1D4)	1:600	Novocastra
TTF-1	M(8G7G3/1)	1:30	Invitrogen, Carlsbad, CA, USA
CDX2	M(CDX2-88)	1:40	BioGenex
α-inhibin	M(R1)	1:10	Bio-Rad, Hercules, CA, USA
α-methylacyl CoA racemase	M(13H4)	1:1	Biologo, Kronshagen, Germany
PSA	P	1:1000	Dako
β-catenin	M(14)	1:1	Ventana/Roche, Tucson, AZ, USA
hMLH1	M(M1)	1:1	Ventana/Roche
hMSH2	M(G219-1129)	1:1	Ventana/Roche
hMSH6	M(44)	1:1	Ventana/Roche
hPMS2	M(EPR3947)	1:1	Ventana/Roche
Ki67	M(MIB1)	1:50	Dako

P/M: polyclonal/monoclonal; EMA: epithelial membrane antigen; PSA: prostatic specific antigen.